Journal of Catalysis 259 (2008) 183–189

Contents lists available at ScienceDirect

Journal of Catalysis

www.elsevier.com/locate/jcat

Reaction of ethanol over hydroxyapatite affected by Ca/P ratio of catalyst

Takashi Tsuchida [a,*], Jun Kubo [a], Tetsuya Yoshioka [a], Shuji Sakuma [a], Tatsuya Takeguchi [b], Wataru Ueda [b]

[a] Central Research Center, Sangi Co., Ltd., Fudoinno 2745-1, Kasukabe-shi, Saitama 344-0001, Japan
[b] Catalysis Research Center, Hokkaido University, Kita 21 Nishi 10, Kita-ku, Sapporo 001-0021, Japan

ARTICLE INFO

Article history:
Received 18 June 2008
Revised 7 August 2008
Accepted 10 August 2008
Available online 11 September 2008

Keywords:
Hydroxyapatite
Acid basic catalyst
Ca/P ratio
Ethanol
1-Butanol
Guerbet alcohol
Guerbet reaction
Probability
Ethanol activation

ABSTRACT

The mineral hydroxyapatite [HAP; $Ca_{10}(PO_4)_6(OH)_2$] is the chief component of animal bones and teeth. It also is known to function as a catalyst with both acid and base sites, depending on the manner in which it is synthesized. We closely studied the reaction of ethanol over HAP using catalysts of different Ca/P molar ratios. These were prepared by controlling the pH of the solution during precipitation synthesis. We found that the distribution of acid sites and basic sites on the catalyst surface varied with the Ca/P ratio of HAP. The yields of ethylene, 1-butanol, and 1,3-butadiene were correlated with the ratio of acid sites and basic sites. We further found that yields of higher alcohols, such as 1-butanol, that are known as Guerbet alcohols and are characteristic products of ethanol over HAP, are functions of the probability of ethanol activation (α) on the catalyst surface.

1. Introduction

Hydroxyapatite [HAP; $Ca_{10}(PO_4)_6(OH)_2$] is the main component of animal bones and teeth. It is used widely in fields such as bone regeneration, dental materials, fertilizers, and food supplements (as a source of calcium). It also is used industrially in sensors, fluorescence materials, chromatography, and environmental phosphorus recovery; its use in drug delivery systems has been well studied [1–3]. As a catalyst, HAP has the unusual property of containing both acid sites and basic sites in a single crystal lattice [4–13]. The stoichiometric form of HAP is shown as $Ca_{10}(PO_4)_6(OH)_2$, and its molar ratio is 1.67. The ionic radius of HAP's component elements allows a fair degree of transfer or loss of ions within its crystal structure [14]. As a result, HAP is a highly nonstoichiometric calcium phosphate compound with a Ca/P molar ratio ranging from 1.50 to 1.67. Joris and Amberg [15] postulated that HAP's nonstoichiometry is facilitated by the fact that the loss of Ca^{2+} ions and resulting electrical imbalance are corrected by introduction of H^+ ions and depletion of OH^- ions, representing this by the formula $Ca_{10-Z}(HPO_4)_Z(PO_4)_{6-Z}(OH)_{2-Z}$; $0 < Z \leqslant 1$. It is known that at a Ca/P ratio of 1.50, highly crystalline HAP acts as an acid catalyst, catalyzing chiefly ethylene synthesis from ethanol by dehydration; however, at a Ca/P ratio of 1.67, it acts as a basic catalyst, catalyzing chiefly acetaldehyde synthesis from ethanol by dehydrogenation. HAP also is known to have the character of both an acid catalyst and a basic catalyst when its Ca/P ratio is between 1.50 and 1.67 [4–7]. However, there has been no quantitative report concerning the reaction of ethanol over highly activated HAP acting as both an acid catalyst and a basic catalyst. From a catalytic standpoint, it is thought that active sites newly emerge on the surface of nonstoichiometric HAP as it loses calcium, phosphoric acid, and hydroxyl groups. We found that we could refine the reaction of ethanol over HAP by using catalysts with different Ca/P molar ratios, which we prepared by controlling the pH of the solution during precipitation synthesis. Our results explain the peculiar distribution of reaction products from ethanol over HAP catalysts.

2. Experimental

2.1. Catalyst preparation

Four HAP catalysts were prepared by the precipitation method. In each case, a solution containing 0.60 mol/l of $Ca(NO_3)_2{\cdot}4H_2O$ and a solution containing 0.40 mol/l of $(NH_4)_2HPO_4$ [16,17] were fed slowly into a container and mixed by stirring for 24 h at 80 °C. The precipitate was then washed with deionized water, filtered, dried at 140 °C and calcined at 600 °C for 2 h in atmosphere. Different levels of nonstoichiometry in the four HAP catalysts were obtained by controlling the pH of the mixture of solutions at 7.0, 9.0, 10.0, and 10.5, using aqueous ammonia. CaO and MgO were used as representative base catalysts for comparison; these were

* Corresponding author. Fax: +81 48 752 0120.
E-mail address: takashi.tsuchida@sangi-j.co.jp (T. Tsuchida).

0021-9517/$ – see front matter
doi:10.1016/j.jcat.2008.08.005

synthesized from materials purchased from Wako Pure Chemical Industries Inc. CaO was synthesized by dehydration of special-grade $Ca(OH)_2$ at 600 °C for 2 h in air and MgO by dehydration of $Mg(OH)_2$ (0.07 μm) at 500 °C for 30 min in air. β-TCP ($Ca_3(PO_4)_2$) (Taihei Chemical Industrial Co., Ltd.; Ca/P ratio, 1.50), was used as a representative calcium phosphate catalyst.

2.2. Characterization

The catalysts were characterized as follows. Crystal structures were specified by powder X-ray diffraction (XRD) using a model M18XHF22-SRA diffractometer (Mac Science Co., Ltd., now Bruker Japan Co., Ltd.; monochromatized Cu$K\alpha$ radiation; tube voltage, 45 kV; tube current, 300 mA; slit width, DS 1.00°, SS 1.00°, RS 0.30 mm). The morphological appearance of the catalysts was observed by scanning electron microscopy (SEM) using a Hitachi S-4500 scanning electron microscope. Surface areas were measured with a conventional BET nitrogen adsorption apparatus (Coulter SA3100). Bulk Ca/P ratios of HAP were determined by inductively coupled plasma-atomic emission spectrometry (ICP-AES) using a Seiko Instruments SPS1700R device. Surface Ca/P ratios of HAP were determined from the binding energy (BE) of Ca 2p and P 2p by X-ray photoelectron spectroscopy (XPS) using a JEOL JPS-9010MC spectrometer with monochromatized Mg$K\alpha$ radiation. The densities of acid sites and basic sites on the catalysts were measured by temperature-programmed desorption (TPD) using a BEL-CAT (BEL Japan Inc.) equipped with a mass spectrometer. For TPD measurement, 0.1 g of catalyst was used. This was dehydrated at 500 °C for 30 min in a 50-ml/min helium flow, then cooled to 250 °C. Probe gas (5% NH_3/He for acid sites and 5% CO_2/He for basic sites) was then adsorbed for 30 min in a 50-ml/min flow. After purging at the same temperature, the temperature was raised at a rate of 10 °C/min to 1050 °C in a 30-ml/min helium flow. The densities of acid sites and basic sites on the catalysts were determined by mass spectrometry (Q-MS) using an Pfeiffer Vacuum OmniStar spectrometer with peaks of $M/Z = 16$ at around 320 °C for acid sites and $M/Z = 44$ at around 330 °C for basic sites.

2.3. Reaction methods

Ethanol conversion was carried out using 4.0 ml of each respective catalyst (the four HAP catalysts, CaO, MgO, and β-TCP), and the reaction products were analyzed. In each case, catalyst in powder form was placed in a molding machine to form pellets. The pellets were then lightly crushed to a particle size of 14–26 mesh. In each experiment, 16.4 vol% of ethanol gas diluted with helium was passed at 116 ml/min (GHSV: 2000 h^{-1}) through a fixed-bed silica tubular reactor with interior diameter of 5 mm at atmosphere. The reaction products were analyzed by gas chromatography–mass spectrometry (GC-MS) using a Shimadzu GC-MS-QP5000 chromatograph in the range $M/Z = 10$–400 and by GC with a flame ionization detector (GC-FID) using a Shimadzu GC-14A chromatograph. In both cases, columns supplied by J&W Scientific Corporation (liquid phase, DB-1; film thickness, 5.00 μm; column dimensions, 30 m × 0.323 mm) were used. The performance of the reactions (ethanol conversion and product selectivity) was calculated as in our previous work [16,17].

3. Results and discussion

3.1. Characterization of catalysts

Fig. 1 shows XRD patterns for the four HAP catalysts. These findings confirm that all four are composed of crystalline HAP and no other substances. Fig. 2 shows SEM images of the four HAP catalysts. Those with low Ca/P ratios appear rodlike or platelike,

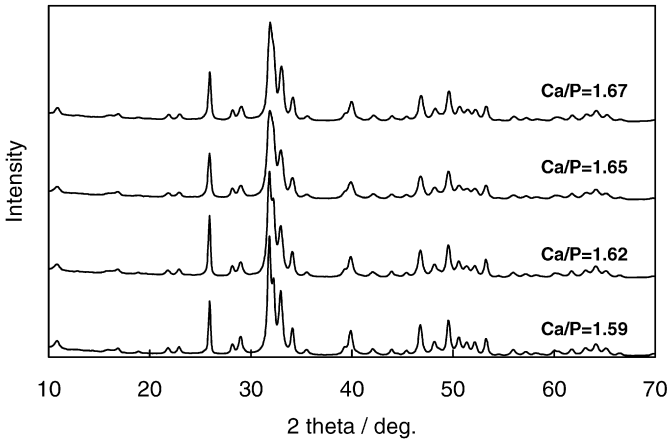

Fig. 1. XRD patterns of the four HAP catalyst powders (calcined at 600 °C for 2 h in atmosphere).

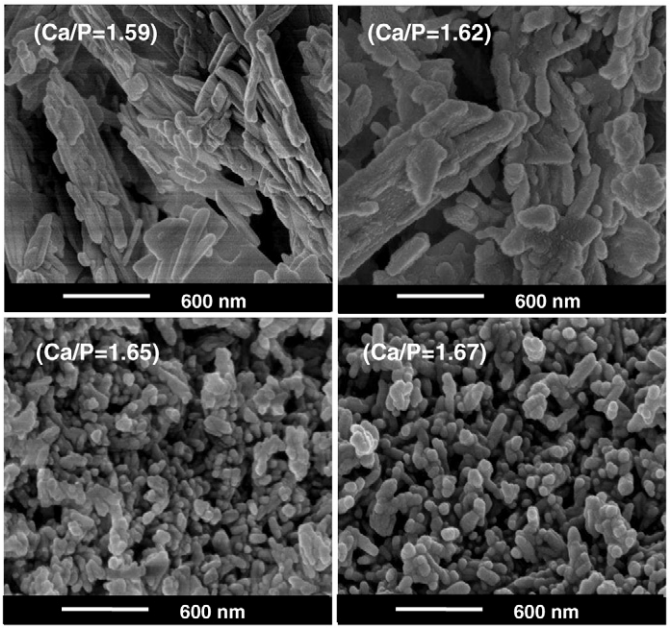

Fig. 2. SEM images of the four HAP catalyst powders (calcined at 600 °C for 2 h in atmosphere).

whereas those with high Ca/P ratios are more nodular and shorter in length. We believe that this difference arises from the process of HAP synthesis, because in precipitation solutions with a low pH, tabular brushite ($CaHPO_4{\cdot}2H_2O$) is precipitated as a precursor and is gradually transformed into HAP [1–3]. Other physical properties of the catalysts (BET surface area and density of acid and basic sites) are summarized in Table 1, which also gives the Ca/P ratio and precipitation suspension pH data for the four HAP catalysts. The fact that the Ca/P ratio of HAP can be changed by controlling the pH of the precipitation solution during synthesis derives from the morphological and electrical stability of phosphate ions (i.e., $H_2PO_4^-$, HPO_4^{2-}, and PO_4^{3-}) in relation to pH. Phosphate ions in solution exist in equilibrium, as shown in (1), and the solubility product indicates that as the pH of the solution rises, the most highly ionized form (PO_4^{3-}) becomes most prevalent [18]:

$$H_3PO_4 \overset{K_1}{\rightleftarrows} H_2PO_4^- \overset{K_2}{\rightleftarrows} HPO_4^{2-} \overset{K_3}{\rightleftarrows} PO_4^{3-},$$

$$K_1 = 7.50 \times 10^{-3}, \quad K_2 = 6.20 \times 10^{-8}, \quad K_3 = 1.70 \times 10^{-12}. \qquad (1)$$

Thus, according to the chemical formula for nonstoichiometric HAP, $Ca_{10-Z}(HPO_4)_Z(PO_4)_{6-Z}(OH)_{2-Z}$; $0 < Z \leqslant 1$, if we want to synthesize HAP with a high Ca/P ratio (i.e., decrease the Z value), then we need to reduce the number of HPO_4^{2-} ions. In other words, we need to raise the pH of the precipitation solution and increase the number of PO_4^{3-} ions.

The results of XPS analysis (Table 1) show that the surface Ca/P ratios of HAP were smaller than the bulk Ca/P ratios. The same tendency was seen in previous studies [19–22]. On the other hand, the surface Ca/P ratio of β-TCP was same as its bulk Ca/P ratio. Because β-TCP is a mineral without nonstoichiometric composition [2,3], we can conclude from the findings that a difference in surface and bulk Ca/P ratios is a unique characteristic peculiar to HAP.

The right column of Table 1 gives the density of acid sites and basic sites on the catalysts. For the four HAP catalysts, the higher the Ca/P ratio, the lower the acid site density; however, acid sites were still present on those catalysts with a high Ca/P ratio. In contrast, basic sites barely existed on the catalysts with a Ca/P ratio $\leqslant$1.62; however, a high basic site density was observed on the catalysts with a Ca/P ratio >1.62. No evidence of acidic properties was observed in CaO and MgO, and only a slight amount was confirmed in β-TCP in our TPD analysis. At around 320 °C, the CaO catalyst also showed no evidence of basic properties, although a larger CO_2 peak than that for HAP was seen above 500 °C. But the MgO and β-TCP catalysts had basic site densities equal to about one-third that of the HAP catalyst with a Ca/P ratio of 1.65 and almost the same as that of the HAP catalyst with a Ca/P ratio of 1.67.

We considered the relationship between the HAP catalysts' Ca/P ratio and their numbers of acid and basic sites in the following manner. It is known that the acid/basic property of nonstoichiometric HAP is governed by its Ca^{2+} ions; that is, its basic property derives from the presence of Ca^{2+} ions, and its acidic property derives from the deficiency of Ca^{2+} ions [1–3]. Moreover, the HAP crystal grows along its c-axis, so that the a-faces, which contain phosphate groups related to acidity, are mainly exposed [23]. The Ca/P ratio is lower at the surface of HAP particles than within their bulk, as our XPS study revealed. This also suggests that HAP's calcium ions, considered related to basic properties, are not readily expressed at the surface level. SEM showed that nonstoichiometric HAP with a Ca/P ratio of $\leqslant$1.62 was morphologically rodlike or platelike. We concluded that in this case, the phosphate-bearing a-faces were largely exposed and surface expression of calcium was limited, resulting in a relatively high density of acid sites. In contrast, SEM showed that HAP with a Ca/P ratio of $\geqslant$1.65 (i.e., at or close to stoichiometric composition) was more globular and compact. We concluded that in this case, HAP's calcium-bearing c-faces were more highly exposed, resulting in the high basic site density that was confirmed by our TPD analysis.

Table 1
Characteristic properties of catalysts

Catalyst	pH[a]	Ca/P molar ratio		Z[b]	BET (m^2/g)	Density[c] (μmol/m^2) of	
		Bulk[d]	Surface[e]			Acid sites	Basic sites
HAP-1	7.0	1.59	1.40	0.46	27.5	0.038	0.01
HAP-2	9.0	1.62	1.43	0.28	35.7	0.029	0.02
HAP-3	10.0	1.65	1.44	0.10	40.3	0.011	0.38
HAP-4	10.5	1.67	1.50	0.00	37.8	0.006	0.53
CaO[f]	–	–	–	–	6.4	0.000	0.00
MgO[g]	–	–	–	–	166.0	0.000	0.13
β-TCP	–	1.50	1.50	–	1.2	0.008	0.60

Note. HAP: Hydroxyapatite, TCP: tricalcium phosphate ($Ca_3(PO_4)_2$).
[a] pH of precipitation suspension during catalyst synthesis.
[b] Amount of Ca loss in the formula $Ca_{10-Z}(HPO_4)_Z(PO_4)_{6-Z}(OH)_{2-Z}$; $0 < Z \leqslant 1$ [15].
[c] Data measured by TPD. Probe gas was adsorbed at 250 °C.
[d] Molar ratio determined with ICP.
[e] Molar ratio determined from XPS.
[f] At around 320 °C, the CaO catalyst showed no evidence of basic properties although a larger CO_2 peak than for HAP was measured at above 500 °C.
[g] MgO was calcined at 500 °C for 0.5 h in atmosphere, and other catalysts at 600 °C for 2 h in atmosphere.

3.2. Catalytic reaction

Table 2 shows the selectivities (C wt%) of main reaction products from ethanol at 10% and 20% conversion. Only a trace of the C_1 product methane was formed on all catalysts evaluated, indicating that ethanol was not decomposed on them. The change in the

Table 2
Main product selectivities at 10% and 20% conversion of ethanol on catalysts (contact time 1.78 s). Selectivity was calculated by Arrhenius plot using the experimental data

Catalyst	HAP-1		HAP-2		HAP-3		HAP-4		CaO		MgO		β-TCP	
Ca/P molar ratio	1.59		1.62		1.65		1.67		–		–		1.50	
Conversion (%)	10.0	20.0	10.0	20.0	10.0	20.0	10.0	20.0	10.0	20.0	10.0	20.0	10.0	20.0
Areal rate (μmol/(m^2 s)) × 10^{-3}	42	84	29	58	20	40	19	38	85	170	7	14	367	735
Reaction temp. (°C)	371	387	320	350	275	296	272	298	397	421	352	385	405	436
Selectivity (C wt%)														
CH_4	0.0	0.0	0.0	0.0	0.0	0.0	0.0	0.0	0.2	0.3	0.1	0.1	0.1	0.1
$CH_2{=}CH_2$	82.4	87.3	7.7	16.7	0.9	1.0	0.5	0.6	55.1	57.0	18.2	20.8	15.7	22.9
(TOF) (s^{-1}) × 10^{-3}	*910*	*1929*	*77*	*332*	*16*	*36*	*16*	*37*	–	–	–	–	*7671*	*22,470*
CH_3CHO	4.8	3.4	7.0	4.9	2.9	1.7	2.2	1.7	26.5	18.7	8.8	6.9	21.0	18.6
$(CH_3)_2CO$	0.0	0.0	0.0	0.0	0.0	0.0	0.0	0.0	0.0	1.4	0.0	0.7	0.1	0.1
1,3-butadiene	0.0	0.0	4.9	13.8	1.0	1.1	0.7	0.8	0.5	0.4	4.4	5.1	2.8	4.6
C_4 olefins	0.2	0.2	1.8	3.2	1.0	0.5	0.5	0.3	1.6	1.5	1.2	1.0	1.3	1.1
$C_4^{=}$ aldehydes[a]	0.0	0.0	0.7	0.6	0.2	0.1	0.2	0.1	0.0	0.0	0.5	0.8	1.2	1.3
Butyraldehyde	0.0	0.0	0.4	0.4	0.2	0.3	0.2	0.2	0.4	0.9	0.2	0.4	0.8	1.3
$C_4^{=}$ OHs[b]	0.0	0.0	12.6	5.6	6.8	5.1	5.4	3.5	0.0	0.0	11.3	10.3	10.2	7.0
$C_2H_5OC_2H_5$	12.3	8.8	2.2	2.2	0.4	0.4	0.2	0.2	0.0	0.0	0.0	0.0	9.9	9.6
1-C_4H_9OH	0.0	0.0	49.6	39.2	67.3	68.8	70.7	69.8	2.7	2.3	31.3	27.9	29.5	25.6
(TOF) (s^{-1}) × 10^{-3}	*0.6*	*1.3*	*595*	*941*	*35*	*72*	*25*	*50*	–	–	*17*	*30*	*181*	*314*
$C_2H_5CH(C_2H_5)CH_2OH$	0.0	0.0	2.8	1.7	6.5	6.5	7.4	7.0	0.1	0.1	0.7	1.1	0.3	0.3
1-$C_6H_{13}OH$	0.0	0.0	1.6	1.9	3.1	5.0	3.8	5.8	0.1	0.1	1.2	1.7	0.7	1.0
$C_4H_9CH(C_2H_5)CH_2OH$	0.0	0.0	0.2	0.2	0.6	1.0	0.7	1.1	0.0	0.0	0.2	0.3	0.0	0.0
1-$C_8H_{17}OH$	0.0	0.0	0.1	0.1	0.2	0.5	0.2	0.6	0.0	0.0	0.1	0.2	0.0	0.0
Aromatics	0.0	0.0	0.1	0.1	0.0	0.2	0.2	0.5	0.4	1.0	1.3	2.2	0.1	0.2
Others	0.3	0.3	8.5	9.4	8.8	7.8	7.2	7.7	12.4	16.3	20.7	20.6	6.3	6.0

[a] Unsaturated C_4 aldehydes.
[b] Unsaturated C_4 alcohols.

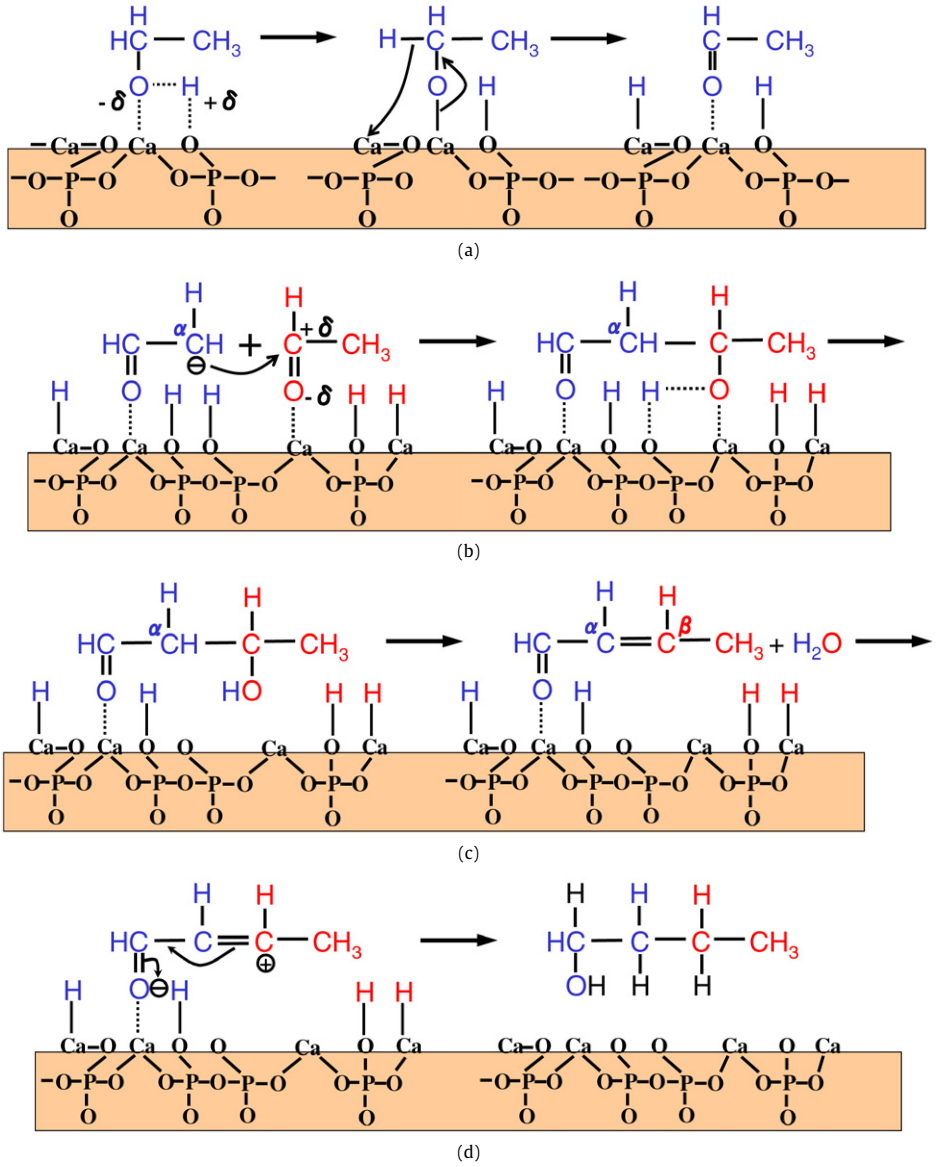

Scheme 1. 1-Butanol formation mechanism in ethanol conversion reaction (a) activation of ethanol (aldehyde formation); (b) aldol condensation; (c) dehydration of aldol; (d) hydrogenation of unsaturated aldehyde.

ethanol conversion rate had almost no effect on product selectivity for any of the catalysts, except for the fact that the selectivity of ethylene increased and that of acetaldehyde decreased for all catalysts with increasing ethanol conversion. At 20% ethanol conversion, for instance, ethylene selectivity was 87.3% on HAP with Ca/P = 1.59 (HAP-1), 57.0% on CaO, 22.9% on β-TCP, 20.8% on MgO, 16.7% on HAP with Ca/P = 1.62 (HAP-2), 1.0% on HAP with Ca/P = 1.65 (HAP-3), and 0.6% on HAP with Ca/P = 1.67 (HAP-4). Diethylether selectivity was 8.8%, and the combined selectivity of ethylene and diethylether was 96.1% on HAP-1; thus, this catalyst is considered a typical solid acid catalyst. In contrast, acetaldehyde selectivity at 20% ethanol conversion was 18.7% on CaO, 18.6% on β-TCP, 6.9% on MgO, 4.9% on HAP-2, 3.4% on HAP-1, and 1.7% on HAP-3 and HAP-4. We had expected to find much higher selectivity to acetaldehyde on CaO, which is a typical basic catalyst. We suggest that this relatively low selectivity to acetaldehyde on CaO under the reaction conditions used resulted from the fact that dehydration of ethanol occurred predominantly at the high reaction temperature of 421 °C. Selectivity to 1-butanol was 69.8% on HAP-4, 68.8% on HAP-3, 39.2% on HAP-2, 27.9% on MgO, 25.6% on β-TCP, 2.3% on CaO, and undetectable on HAP-1.

Turnover frequency (TOF) for ethylene synthesis and 1-butanol synthesis is also given in Table 2. We supposed that ethanol was converted to ethylene on the catalysts' acid sites and to 1-butanol on their basic sites. We defined TOF as the number of ethanol molecules converted per active site per second and calculated it by using the values for density of acid sites and basic sites on the catalysts given in Table 1. Comparing the TOF results shows that ethylene synthesis (i.e., dehydration of ethanol) was more predominant on HAP without basic sites than on HAP with both acid sites and basic sites. In contrast, HAP with basic sites had higher TOF values than MgO in 1-butanol synthesis, suggesting that HAP catalysts with basic sites synthesize 1-butanol more effectively than MgO.

We can explain the difference in 1-butanol synthesis between MgO and HAP as follows. A reaction that synthesizes higher alcohols from lower alcohols (including ethanol) is known as a Guerbet reaction [24–32]. In our proposed mechanism, Guerbet alcohols are synthesized via the aldol condensation of two aldehydes generated by the dehydrogenation of alcohol. Our proposed mechanism for 1-butanol synthesis from ethanol over HAP is shown in Scheme 1. By dissociative adsorption of ethanol in the vapor phase, an ethox-

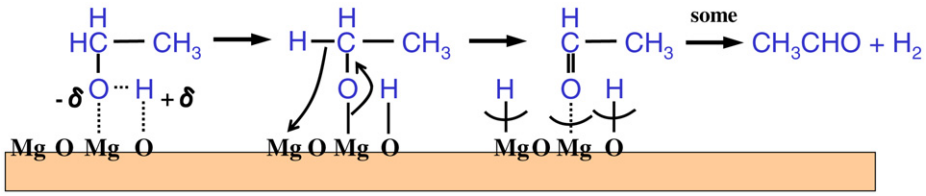

Scheme 2. Dehydrogenation mechanism from ethanol on MgO catalyst.

ide intermediate is adsorbed on Lewis acid sites, and proton-like hydrogen is adsorbed on Brönsted basic sites. The ethoxide is then dissociated into an aldehyde intermediate and hydride-like hydrogen (a). Next, one of two neighboring aldehyde intermediates is decomposed to an enolate (carbanion intermediate), which reacts with the other aldehyde intermediate to form aldol (aldol condensation) (b). Unsaturated aldehyde is then generated by dehydration of the aldol (c), and, finally, 1-butanol is synthesized via hydrogenation of the unsaturated aldehyde (hydride reduction) (d), taking up hydrogen generated by dissociative adsorption during steps (a) and (b).

Our results indicate that the nature of hydrogen adsorption on HAP and MgO differs slightly. As shown in Table 1, on TPD analysis, a peak was observed for MgO at around 320 °C, similar to the peaks observed for HAP-3 and HAP-4. This suggests that like those catalysts, MgO has basic sites. But MgO showed much higher selectivity to acetaldehyde and unsaturated alcohols than any of the HAP catalysts (see Table 2). Our hypothesis to explain this finding is illustrated in Scheme 2. In the case of MgO (Mg-O distance, 0.210 nm), ethanol was dissociatively adsorbed to ethoxide on Mg (Lewis acid sites) and to proton-like hydrogen on ionically bound O (hard basic sites) near these acid sites. This ethoxide then dissociated into aldehyde and hydride-like hydrogen. But because of the short distance between them, the released hydrogen entities, rather than being trapped on the catalyst surface, migrated to form H_2 molecules. These H_2 molecules desorbed into the gas phase with a certain probability. In contrast, in the case of HAP (Ca–O distance, 0.239 and 0.240 nm), we postulate that ethanol was dissociatively adsorbed to ethoxide on Ca (Lewis acid sites) and to proton-like hydrogen on covalently bound O in phosphate groups (soft basic sites) near the acid sites. Dissociative adsorption there resulted in the formation of stable hydrogen phosphate groups. The ethoxide then dissociated into aldehyde and hydride-like hydrogen. We postulated that in the case of the HAP catalyst, there was sufficient distance between the hydrogen entities released during dissociative adsorption for them to become trapped on the catalyst surface without migrating to form molecular hydrogen in the gas phase. As a result, yields of Guerbet alcohols (which are saturated alcohols) were higher on HAP than on MgO.

Although β-TCP, like HAP, has PO_4^{3-} ions, it cannot take a non-stoichiometric form, as HAP can, and cannot trap hydrogen as HPO_4^{2-}. Thus, we concluded that hydrogen migrated more easily to form molecular hydrogen, and acetaldehyde was more readily synthesized, on the β-TCP catalyst surface than on HAP.

Fig. 3 shows the relationship between the Ca/P ratio of HAP catalysts and selectivity to ethylene, 1,3-butadiene, and Guerbet alcohols (total C_4, C_6, C_8, and C_{10} alcohols) at 50% ethanol conversion. Ethylene was the main product when the Ca/P ratio of the catalysts was low, as we reported previously [16]. But ethylene selectivity fell to about 5% when HAP catalysts with higher Ca/P ratios were used. This tendency closely reflected the relationship between the acid site density and Ca/P ratio of the HAP catalysts given in Table 1. On the other hand, Guerbet alcohols were not synthesized at all over the HAP catalyst with the lowest Ca/P ratio and were synthesized only to a small degree over HAP with a Ca/P ratio of 1.62. But Guerbet alcohols were the main products of

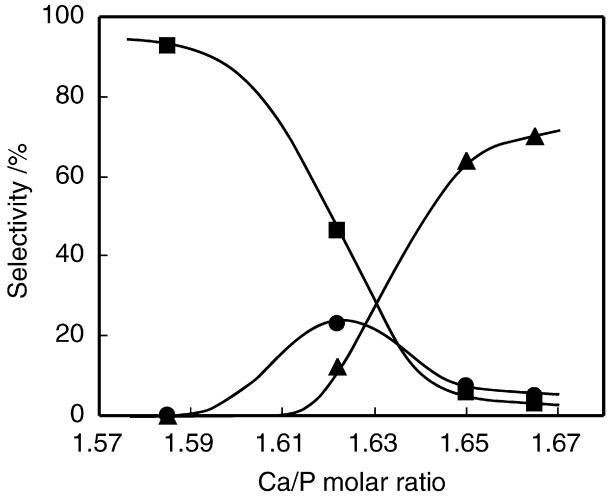

Fig. 3. Selectivity of main products at 50% conversion of ethanol: (▲) total Guerbet alcohols, (●) 1,3-butadiene, (■) ethylene. Reaction conditions: catalyst, 4 ml; GHSV, 2000 h^{-1}.

ethanol conversion over HAP catalysts with high Ca/P ratios. This tendency reflects the relationship between the basic site density and Ca/P ratio of the HAP catalysts, also shown in Table 1. We conclude that HAP is a unique catalyst that synthesizes mainly Guerbet alcohols at high Ca/P ratios. In contrast, we found that CaO, a well-known base catalyst, synthesizes mainly ketones and ethylene at 50% ethanol conversion (data not shown). Both CaO and HAP have Ca–O bonds, but their reaction products differ. As seen in Table 1, CaO has neither acid nor basic properties at around 320 °C, as HAP does, but exhibits basic properties only at higher temperature. These data indicate that the reaction of ethanol on HAP catalysts differs greatly from that on CaO catalysts.

1,3-Butadiene was not synthesized at all on HAP-1, which had a low Ca/P ratio of 1.59, and was synthesized to only a small degree on HAP-3 and HAP-4, which had the highest Ca/P ratios. Maximum selectivity for 1,3-butadiene was in fact observed over HAP-2, which had a Ca/P ratio of 1.62, the level at which a relative balance of acid and basic sites was seen on the HAP catalyst (Table 1). The reaction in which 1,3-butadiene is synthesized from ethanol on an acid-base catalyst is known as the Lebedev reaction [33–37]. We postulated that synthesis of 1,3-butadiene from ethanol over HAP with a Ca/P ratio of $\geqslant$1.62 was due to a Lebedev reaction, because over that Ca/P range, HAP showed both acid and basic properties, albeit to a decreasing degree. Other products not shown in Fig. 3 were olefins, aldehydes, dienes, and aromatics. At higher conversion of ethanol (i.e., higher reaction temperature), selectivity to these products increased, resulting in a multicomponent composition that resembled gasoline [17].

3.3. Scheme of Guerbet alcohol synthesis and distribution

As indicated above, our results demonstrate that the Guerbet reaction plays a major role in ethanol conversion over HAP catalysts. We attempted to explain the scheme of Guerbet alcohol

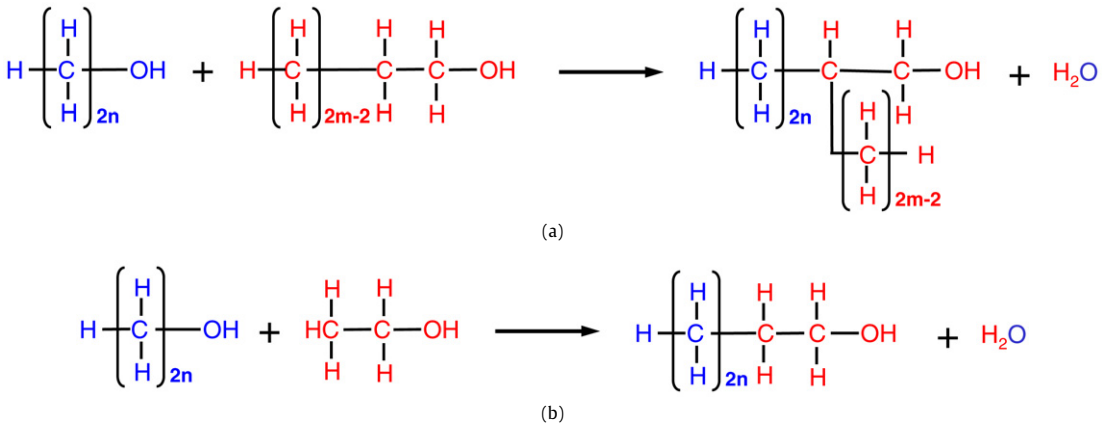

Scheme 3. General formula for the synthesis of Guerbet alcohols from normal alcohols ($m, n \geqslant 1$ and natural numbers). *Note*: The above represents the standard case, in which a branched Guerbet alcohol is formed. When one of the normal alcohols is an enolate derived from ethanol, where $m = 1$ as shown below, the Guerbet alcohol synthesized is a normal alcohol.

Table 3
Synthesis of C_{2n} Guerbet alcohol from normal alcohols during ethanol conversion over HAP, showing type of alcohol synthesized, and generation probability

Carbon number of Guerbet alcohol	Combination of normal alcohols[a]		Type of Guerbet alcohol	Probability
4 ($n = 2$)	(2, 2)	→	normal-	α^2
6 ($n = 3$)	(2, 4)	→	branched-	α^3
	(4, 2)	→	normal-	
8 ($n = 4$)	(2, 6)	→	branched-	α^4
	(4, 4)	→	branched-	
	(6, 2)	→	normal-	
10 ($n = 5$)	(2, 8)	→	branched-	α^5
	(4, 6)	→	branched-	
	(6, 4)	→	branched-	
	(8, 2)	→	normal-	

Note. α: probability of ethanol activation. n: number of ethanol molecules activated.
[a] Combinations in parentheses show carbon numbers for the respective normal alcohols (aldehyde on the left, and enolate on the right) that combine to form Guerbet alcohols. Note that when the enolate's carbon number is 2, a normal Guerbet alcohol is formed.

synthesis over HAP by means of a new concept—namely, the probability of ethanol activation (α) on the catalyst surface. Scheme 3 shows the general formula for synthesis of Guerbet alcohols from two lower alcohols. Generally, Guerbet alcohols synthesized from normal alcohols are branched alcohols. There is an interesting exception to this, however. When one of the normal alcohols is an enolate derived from ethanol, whose carbon number is 2, then $m = 1$ in the formula shown in Scheme 3, and the Guerbet alcohol synthesized ($C_{2n+2}H_{4n+5}OH$) is a normal alcohol whose carbon number is two carbons higher than that of the original normal alcohol ($C_{2n}H_{4n+1}OH$). On the basis of the above, we propose the following two-part hypothesis for synthesis of Guerbet alcohols from ethanol over HAP when ethanol conversion is low:

(1) Some molecules of ethanol are activated and react. (We defined the probability of this activation as α.)
(2) Only normal alcohols react to synthesize Guerbet alcohols.

Table 3 shows the combinations of normal alcohols that synthesize C_{2n} Guerbet alcohols, the type of Guerbet alcohols synthesized (normal or branched), and the probability of such Guerbet alcohols being generated according to the foregoing hypothesis. The combination of normal alcohols (the carbon numbers of which are shown in left–right juxtaposition in Table 3) is explained as follows. Taking the synthesis of C_6 Guerbet alcohols as an example, (2, 4) indicates that an aldehyde sourced from ethanol (carbon number 2) reacts with an enolate sourced from 1-butanol (carbon number 4) to synthesize a branched C_6 Guerbet alcohol, and (4, 2) indicates that an aldehyde sourced from 1-butanol (carbon number 4) reacts with an enolate sourced from ethanol (carbon number 2) to synthesize a normal C_6 Guerbet alcohol. In each group of Guerbet alcohols that share the same carbon number, a normal Guerbet alcohol is generated only when the enolate is derived directly from ethanol and has a carbon number of 2. As the table shows, the ratio of normal to branched Guerbet alcohol generated in each group decreases as the carbon number of the group increases. The probability of generating Guerbet alcohols, both normal and branched, with a carbon number of $2n$ thus can be expressed as α^n, where α is the probability of ethanol activation. Summing up the foregoing relations, the total yields of C_{2n} normal and branched Guerbet alcohols can be expressed by the following general formula:

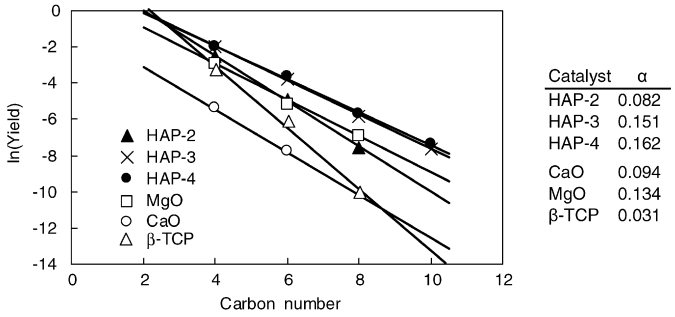

Fig. 4. Yields of Guerbet alcohols by carbon number at 20% conversion of ethanol on β-TCP, MgO, CaO, and HAP catalysts with Ca/P molar ratios of 1.62, 1.65 and 1.67. The right column shows the probability of ethanol activation (α) on each catalyst. Contact time, 1.78 s.

Total yields of Guerbet alcohols

$$= \sum_{n=2}^{\infty} \left\{ \frac{1}{n-1} C\alpha^n + \left(1 - \frac{1}{n-1}\right) C\alpha^n \right\}, \quad \text{where } C\text{: constant.}$$

Here the first and second terms show the yield of normal Guerbet alcohols and branched Guerbet alcohols, respectively.

Fig. 4 illustrates the distribution of Guerbet alcohols synthesized during ethanol conversion over CaO, MgO, β-TCP, and three kinds of HAP catalyst at a conversion rate of 20%, and shows the relationship between yield and carbon number for these alcohols. The lowest line shows data obtained using a CaO catalyst, which synthesized only a small yield of Guerbet alcohols. We believe that selectivity to Guerbet alcohols over CaO was low because other

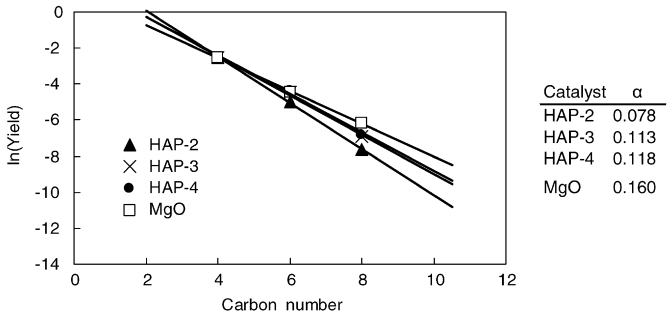

Fig. 5. Yields of Guerbet alcohols by carbon number at 8% yield of 1-butanol (all lines cross here) on MgO and HAP catalysts with Ca/P molar ratios of 1.62, 1.65 and 1.67. The right column shows the probability of ethanol activation (α) on each catalyst. Contact time, 1.78 s.

parallel reactions occurring on the catalyst (e.g., dehydration, dehydrogenation, and the Lebedev reaction) took precedence over the Guerbet reaction. The exponent of the slopes shown in the figure was α, and the smaller the slope, the larger the α value and the greater the yield of Guerbet alcohols. Although the α value for each catalyst was different, the linearity of the slopes indicated that our hypothesis satisfied all of the experimental data obtained for synthesis of Guerbet alcohols on these catalysts. In other words, it supported our hypothesis that at the level of ethanol conversion used in our study, the yield of Guerbet alcohols is regulated by the degree of activation of surface ethanol.

As shown in Table 1, the density of basic sites on catalysts HAP-2, -3, -4 and MgO was 0.024, 0.382, 0.534, and 0.133 μmol/m^2, respectively. As shown in Fig. 4, the probability of ethanol activation (α) for the same four catalysts was 0.082, 0.151, 0.162 and 0.134. This data confirmed that for catalysts HAP-2, -3, -4, and MgO, the probability of ethanol activation over each catalyst increased with the catalyst's basic site density at the same ethanol conversion rate. In addition, based on the data in Fig. 4, we postulate that the catalysts' α values reflect the difference in the number of active sites contributing to the Guerbet reaction for each catalyst at the same ethanol conversion rate. To confirm the character of the active sites that synthesize only Guerbet alcohols, we therefore compared the distribution of Guerbet alcohols synthesized from ethanol over HAP at the point in each reaction where the yield of 1-butanol was 8%; these data are shown in Fig. 5. (In the case of CaO and β-TCP, data were excluded, because the yield of 1-butanol did not reach 8%.) We postulate that the high α value of MgO (0.160) can be explained as follows. An aldehyde deriving from 1-butanol participates in the reaction as a regular basic intermediate, causing the density of 1-butanol on the catalyst to decrease and the ratio of higher Guerbet alcohols to increase, resulting in a high estimated α value. HAP-3 and HAP-4 had roughly the same α value (0.113 and 0.118, respectively), indicating their virtually identical ability to catalyze the synthesis of Guerbet alcohols from ethanol. The α value of HAP-2 was lower, at 0.078. We conclude that for HAP-2, activated ethanol was taken up in a Lebedev reaction (diene synthesis, as indicated in Table 2), so that synthesis of higher Guerbet alcohols on HAP-2 was restrained.

4. Conclusion

Our findings indicate that HAP catalysts, without the addition of noble metals, transition metals, or halogens, such as chlorine, can be used for the highly selective synthesis of valuable compounds, such as 1-butanol and 1,3-butadiene, from ethanol merely by controlling the catalyst's Ca/P molar ratio. We found that product selectivity bore a strong correlation to the acid and basic properties of the HAP catalysts. In seeking to explain the characteristic synthesis of Guerbet alcohols from ethanol on HAP catalysts, we compared the catalysts' acid and basic properties with those of traditional base catalysts CaO and MgO. Based on our findings, we can state the following conclusions:

1. Distribution of higher alcohols from ethanol over HAP by the Guerbet reaction can be expressed with simple probability.
2. Yields of Guerbet alcohols over HAP can be quantitatively expressed as a function of the probability of activation (α) of the raw material, ethanol.
3. α values differ for different catalysts and are influenced by the degree of parallel reactions on the catalyst.
4. α values are correlated with the catalysts' basic site density.

Acknowledgments

We thank the New Energy and Industrial Technology Development Organization (NEDO) of Japan, which provided financial assistance for this research. We also thank Dr. Roslyn Hayman for advice.

References

[1] H. Aoki, Medical Applications of Hydroxyapatite, Ishiyaku EuroAmerica, Inc. Tokyo, St. Louis, 1994, p. 1.
[2] J.C. Elliott, Structure and Chemistry of the Apatites and Other Calcium Orthophosphates, Elsevier Science B.V., Amsterdam, 1994, p. 1.
[3] T. Kanazawa, Inorganic Phosphate Materials, Kodansha, Tokyo, 1989, p. 15.
[4] L.C. Kibby, K.W. Hall, J. Catal. 31 (1973) 65.
[5] J.S. Joris, H.C. Amberg, J. Phys. Chem. 75 (1971) 3167.
[6] F. Nozaki, T. Sodesawa, Hyoumen (in Japanese) 23 (1985) 399.
[7] H. Monma, Syokubai (in Japanese) 27 (1985) 237.
[8] S.A.J. Bett, K.W. Hall, J. Catal. 10 (1968) 105.
[9] L.C. Kibby, K.W. Hall, J. Catal. 29 (1973) 144.
[10] H. F-Milhofer, V. Hlady, F.S. Baker, R.A. Beebe, N.W. Wikholm, J.S. Kittelberger, J. Colloid Interface Sci. 70 (1979) 1.
[11] N.S. Resende, M. Nele, V.M.M. Salim, Thermochim. Acta 451 (2006) 16.
[12] N. Elazarifi, A. Ezzamarty, J. Leglise, L.C. Menorval, C. Moreau, Appl. Catal. A Gen. 267 (2004) 235.
[13] A. Venugopal, M.S. Scurrell, Appl. Catal. A Gen. 245 (2003) 137.
[14] R.E. Kreidler, A.F. Hummel, Am. Mineral. 55 (1970) 170.
[15] J.S. Joris, H.C. Amberg, J. Phys. Chem. 75 (1971) 3167.
[16] T. Tsuchida, S. Sakuma, T. Takeguchi, W. Ueda, Ind. Eng. Chem. Res. 45 (2006) 8634.
[17] T. Tsuchida, T. Yoshioka, S. Sakuma, T. Takeguchi, W. Ueda, Ind. Eng. Chem. Res. 47 (2008) 1443.
[18] A.K. Lynn, W. Bonfield, Acc. Chem. Res. 38 (2005) 202.
[19] S. Sugiyama, T. Miyamoto, H. Hayashi, J.B. Moffat, J. Mol. Catal. A Chem. 135 (1998) 199.
[20] H.B. Lu, C.T. Camphell, D.J. Graham, B.D. Ratner, Anal. Chem. 72 (2000) 2886.
[21] K. Kieswetter, T.W. Bauer, S.A. Brown, F.V. Lente, K. Merritt, Biomaterials 15 (1994) 183.
[22] M. Yoshinari, Y. Ohtsuka, T. Derand, Biomaterials 15 (1994) 529.
[23] H. Aoki, Hyoumenkagaku (in Japanese) 10 (1989) 14.
[24] J.P. Wibaut, US Patent 1 910 582 (1933), to Naamlooze Vennootschap de Bataafsche Petroleum Maatschappij.
[25] R.T. Clark, C.C. Tex, US Patent 3 972 952 (1976), to Celanese Corporation.
[26] W. Ueda, T. Kuwabara, T. Ohshida, Y. Morikawa, J. Chem. Soc. Chem. Commun. (1990) 1558.
[27] W. Ueda, T. Ohshida, T. Kuwabara, Y. Morikawa, Catal. Lett. 12 (1992) 97.
[28] M. Xu, M.J.L. Gines, A.-M. Hilmen, B.L. Stephens, E. Iglesia, J. Catal. 171 (1997) 130.
[29] M.L.J. Gines, E. Iglesia, J. Catal. 176 (1998) 155.
[30] J.I.D. Cosimo, C.R. Apesteguia, M.J.L. Gines, E. Iglesia, J. Catal. 190 (2000) 261.
[31] C. Carlini, M. Marchionna, M. Noviello, R.M.A. Galletti, G. Sbrana, F. Basile, A. Vaccari, J. Mol. Catal. A Chem. 232 (2005) 13.
[32] V.K. Diez, C.R. Apesteguia, J.I.D. Cosimo, J. Catal. 240 (2006) 235.
[33] B.B. Corson, E.H. Jones, E.C. Welling, A.J. Hinckley, E.E. Stahly, Ind. Eng. Chem. 42 (1950) 359.
[34] K.S. Bhattacharyya, D.N. Ganguly, J. Appl. Chem. 12 (1962) 97.
[35] K.S. Bhattacharyya, D.N. Ganguly, J. Appl. Chem. 12 (1962) 105.
[36] R. Ohnishi, T. Akimoto, K. Tanabe, J. Chem. Soc. Chem. Commun. (1985) 1613.
[37] Y. Kitayama, M. Satoh, T. Kodama, Catal. Lett. 36 (1996) 95.